

# Sensitivity of an image plate system in the XUV (60 eV < E < 900 eV)

---

**B.H. Faylor,<sup>a,1</sup> E.M. Gullikson,<sup>b</sup> N.G. Link,<sup>a</sup> J.C. Riordan<sup>a</sup> and B.C. Wilson<sup>c</sup>**

<sup>a</sup>*L-3 Applied Technologies, Pulse Sciences, Inc.,  
2700 Merced St., San Leandro, CA 94577, U.S.A.*

<sup>b</sup>*Lawrence Berkeley National Laboratory,  
1 Cyclotron Road, Berkeley, CA 94720, U.S.A.*

<sup>c</sup>*Defense Threat Reduction Agency,  
Fort Belvoir, VA 22060-6201, U.S.A.*

ABSTRACT: Phosphor imaging plates (IPs) have been calibrated and proven useful for quantitative x-ray imaging in the 1 to over 1000 keV energy range. In this paper we report on calibration measurements made at XUV energies in the 60 to 900 eV energy range using beamline 6.3.2 at the Advanced Light Source at Lawrence Berkeley National Laboratory. We measured a sensitivity of  $\sim 25 \pm 15$  counts/pJ over the stated energy range which is compatible with the sensitivity of Si photodiodes that are used for time-resolved measurements. Our measurements at 900 eV are consistent with the measurements made by Meadowcroft et al. at  $\sim 1$  keV.

---

## Contents

<b>1</b>	<b>Introduction</b>	<b>1</b>
<b>2</b>	<b>Technical approach</b>	<b>1</b>
<b>3</b>	<b>Experiments and results</b>	<b>2</b>
<b>4</b>	<b>Conclusions</b>	<b>5</b>

---

## 1 Introduction

Extreme Ultraviolet (XUV) photons are difficult to image because they interact strongly with most materials. Back illuminated charge-coupled device (CCD) cameras have been used [1], but are limited in active area, are difficult to clean, and the hardware is expensive. XUV sensitive film, such as Kodak 101, which does not have an overcoat, is fragile and requires chemical processing. The Computed Radiography (CR) phosphor imaging plate (IP) is an intriguing alternative because they have a wide number of applications, from medical radiography (the application that drove their initial development) to plasma spectroscopy research [2] due to their (1) large linear dynamic range,  $\sim 10^5$ , (2) low cost,  $< \$1000$ , (3) availability in large areas,  $\sim 30$  cm, and (4) sensitivity which is compatible with Si photodiodes. Some imaging plates have been engineered to efficiently detect beta-particles from tritium. One such plate is the “Kodak Storage Phosphor Screen TR” (Ref. 1041540). Meadowcroft et al. have previously reported on the sensitivity and fading characteristics of IPs for 1–75 keV x rays [3]. In this paper we present sensitivity measurements for the “Kodak Storage Phosphor Screen TR” plate in the 60–900 eV energy range, demonstrating that IPs can be successfully used for XUV imaging.

## 2 Technical approach

The IP contains phosphor that can store a latent image which is later digitized by raster scanning its surface with a laser beam and recording the luminescence with a photomultiplier tube (PMT) [3]. We used a plate which had a BaFBr phosphor, activated with Eu, chemical formula BaFBr(Eu). The phosphor was deposited on a flexible plastic substrate and the surface facing the XUV source was protected with a thin layer of cellulose acetate [4]. The IP was digitized using a commercially available scanner [5], and software [6], which allowed the following parameters to be set: (1) scan speed, (2) spatial resolution, and (3) PMT voltage (which determines the PMT gain). PMT voltage directly affects the digitized image pixel value amplitudes and the spatial resolution specifies the length and width of the square pixels. Scan speed determines how rapidly the image is scanned and a slower speed will result in a larger dynamic range because there is more time for an efficient transfer of the stored energy on the plate. The latent image stored on the plate does fade with

time [3], so the time between exposure and digitization needs to be accounted for in order to achieve the highest accuracy possible.

We exposed the IP to XUV radiation at the Advanced Light Source (ALS) at Lawrence Berkeley National Laboratory. Beamline 6.3.2 provides virtually monochromatic ( $E/\Delta E \geq 7000$ ) photons in the energy range of interest, 50–1000 eV [7]. The exposure chamber includes calibrated detectors that allow the XUV flux to be monitored, shutters, apertures and filters for modulating the beam intensity, and a sample stage for positioning the object under test, in our case the IP, in and out of the photon beam.

### 3 Experiments and results

Two days of IP exposures will be described here. The goal of the first day was to get measurements of the IP sensitivity for just a few energies spread over a wide range. During the second day we focused on relatively closely spaced energies at low photon energy ( $E < 100$  eV) and also at the C and O K-edges where we expected to see modulations in sensitivity due to absorption in the cellulose acetate protective layer.

On the first day, two IP exposures were done, one IP at 900 eV followed by a second IP with exposures taken at 100, 185, 400, and 500 eV. By changing a beamline aperture, power levels between  $\sim 0.1$  and  $\sim 100$  nW were achieved. Since the XUV spot size was only  $\sim 100$   $\mu\text{m}$  vertically by  $\sim 300$   $\mu\text{m}$  horizontally, the IP was scanned at an average speed of 0.75 cm/sec in the vertical direction to produce regions of relatively uniform exposure with peak fluences in the 5–5000 nJ/cm<sup>2</sup> range (corresponding to 0.5–500 pJ/pixel for 100  $\mu\text{m}$  square pixels). A range of exposures were used initially because the sensitivity of the image plate to the XUV was unknown. An example of an IP image from the first day is shown in figure 1. The IP scanner settings were 600 V PMT voltage, and a 4000 rpm scan speed. The spatial resolution was held at 100 microns for all the scans reported here. Because the IPs were scanned within 5 minutes of exposure, compensation for fading was not necessary [3].

On the second day of experiments we captured two images. The first exposure explored the low energy range and included exposures at 60, 65, 75, 80, and 100 eV in the vicinity of the Ba M4 and M5 edges. The second exposure was done at 270, 280, 290, 300, 530, 540, 550, and 560 eV, bracketing the C K and O K edges. For this second day, the scan speed was reduced to 2000 rpm. We think that this changes the shape of the exposed lines slightly, but not the integrated values that are reported here. In contrast to the first day, the IPs were not scanned within 5 minutes of exposure, but rather not until 125 to 197 minutes afterwards. Previous experimental measurements [3] for a phosphor without an overcoat indicate a fading time constant of  $\sim 36$  min while a phosphor with an 8 micron overcoat had a measured time constant of  $\sim 57$  min. As shown below, x-ray measurements indicate that the overcoat thickness for the IP described here is well below 1 micron, but even if the longer time constant is used, the fact that the fading component amplitude is just 31% of the total signal [3] means that the maximum error that could be introduced is from 0.8 to 2.5%. Because of its small amplitude, we will neglect the fading component in the discussion that follows. The measured signals for the two IPs exposed on the second day should be 69% of the amplitude that would have been measured if the IP had been scanned within a few minutes of the exposure, rather than 2–3 hours later.

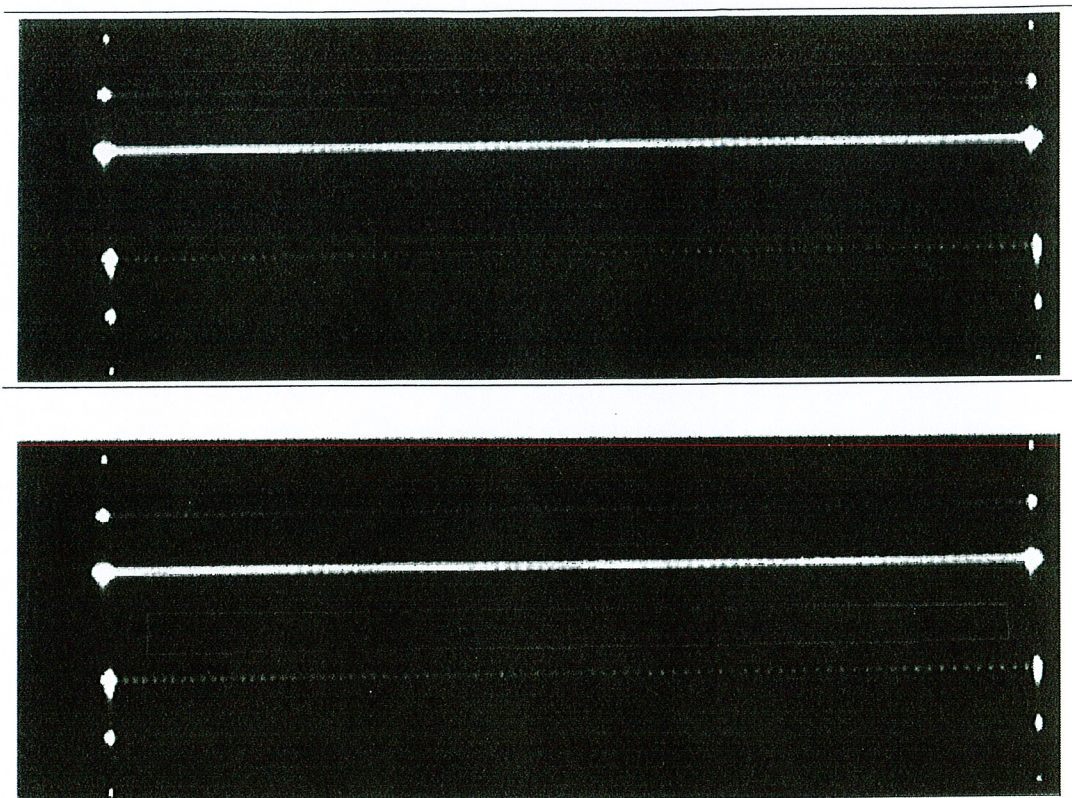


**Figure 1.** During the first day a number of different diameter apertures were used to produce a range of exposures on the IP. Top: region of interest (ROI) over which the image was integrated is outlined in red. This region corresponds to a photon energy of 185 eV and a beamline aperture of 3 mm. Bottom: ROI corresponds to no exposure and will be used for background subtraction. The exposures from top to bottom in this image were separated by 3 mm on the IP and correspond to (1) 185 eV, 1 mm aperture, (2) 185 eV, 3 mm aperture, (3) 185 eV, no aperture ( $\sim 10$  mm diameter opening), (4) no exposure (provides background level), (5) 400 eV, no aperture ( $\sim 10$  mm diameter opening), (6) 400 eV, 3 mm aperture, (7) 400 eV, 1 mm aperture. For the weakest two scans, (1) and (7), only the starting and ending points, where the XUV beam rested between scans, are clearly visible on the images. The scans look nonuniform (like a series of dots) because the stepping mechanism used to position the IP did not move at a constant velocity.

The results for all the sensitivity measurements are given in table 1 and figure 2. Because absolute intensity measurements were available for the first day, and only relative intensity measurements for the second due to a recording error, the second day data is normalized to the first at 100 eV, the only energy common to both days. The reported values were found by (1) integrating an area on the image corresponding to a particular energy exposure, (2) subtracting the integral of the same area in an unexposed region of the image (see example in figure 1), and (3) normalizing by the product of the length of the integral on the IP and the energy deposited per unit length by the ALS.

The effective thickness of the cellulose acetate protective layer can be estimated from the height of the absorption feature corresponding to the C K edge, assuming a slow variation in the phosphor response for the energies 270, 280, 290, and 300 eV. The chemical formula for the cellu-

**Table 1.** Sensitivity data were acquired on two different days. On the first day, the data was absolutely calibrated. Only a relative calibration was obtained on the second day, so the sensitivity measurements for that day have been scaled at the photon energy common to both days — 100 eV.

calibration	photon E (eV)	sensitivity (counts/pJ)
absolute	100	14.60
absolute	185	36.58 ± 0.56
absolute	400	27.23 ± 0.94
absolute	500	36.50 ± 0.28
absolute	900	33.31 ± 9.61
relative	60	11.90 ± 1.17
relative	65	12.30
relative	75	15.94
relative	80	16.50
relative	270	29.40 ± 1.03
relative	280	30.87
relative	290	18.53
relative	300	20.99
relative	530	29.85
relative	540	26.73
relative	550	27.04
relative	560	26.88

lose acetate was not specified, so estimates were made for  $C_6H_2O_2(OH)_3$  and  $C_6H_2O_2(OOCCH_3)_3$ , the two extremes of  $C_6H_2O_2(OH)_{3-m}(OOCCH_3)_m$ ,  $0 \leq m \leq 3$ . The areal densities found from the fits of the natural logarithm of signal versus linear mass absorption coefficient are given in table 2. The areal density value estimate,  $\sim 20 \mu\text{g}/\text{cm}^2$ , is about 50 times lower than the expected thickness based on an application of  $\sim 1 \text{ mg}/\text{cm}^2$  of coating material. At least 3 factors could influence this result. First, the phosphor particles as deposited on the IP backing along with a binder, will form a surface with finite roughness and voids that would wick up the overcoat material, which we assume is applied as a liquid. Secondly, the phosphor particles nearer the surface of the IP would have a higher probability of contributing to the detected signal because they have a higher probability of (1) being stimulated by the readout laser and (2) having their luminescence escape to the IP surface. Finally, when XUV photons produce electrons in the overcoat, phosphor, and binder, the phosphor particles near the surface are most likely to be excited by those electrons and the secondary electrons that they produce.

The sensitivity of the imaging plate is  $\sim 4000$  to  $8000$  times less than the sensitivity of a typical CCD that is directly detecting x rays. Reference 9 reports a digitization setting of 6.55 electrons/count. Assuming 3.65 eV is required to generate an electron in the CCD and a quantum detection efficiency of 0.4–0.8, the sensitivity is  $\sim 100,000$  to  $200,000$  counts/pJ.

The sensitivity of  $\sim 25$  counts/pJ is consistent with the values reported by Meadowcroft et al. for a different IP system. In the low energy limit they reported sensitivities  $\sim 0.5$  “mPSL/keV” [3].

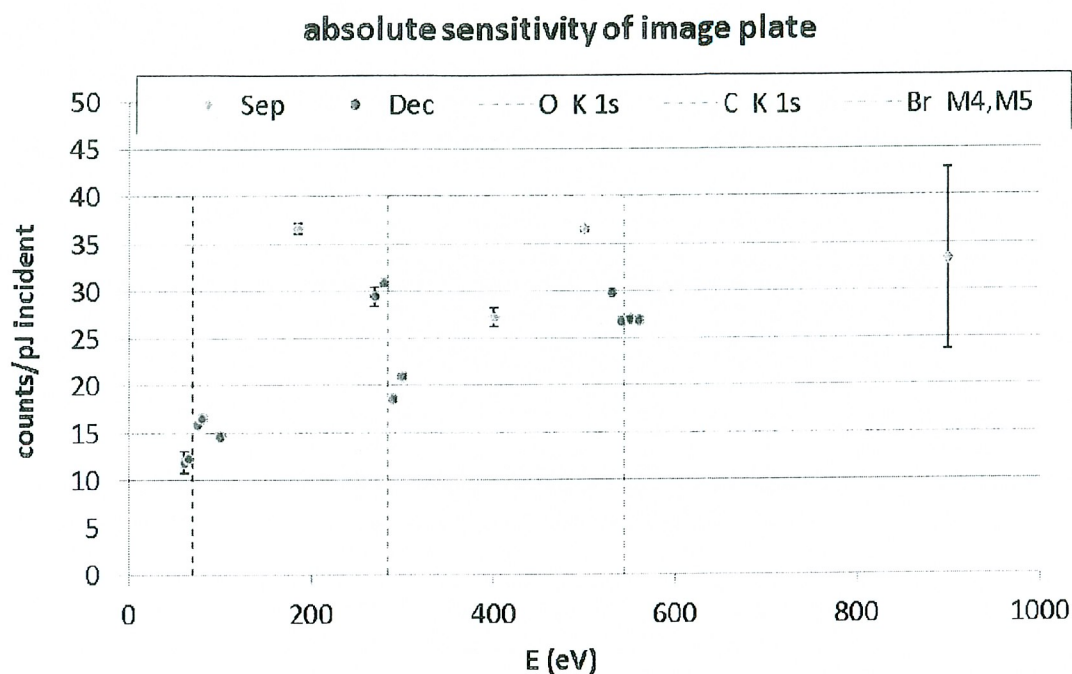


**Figure 2.** The sensitivity of an image plate-image plate scanner combination is  $\sim 25 \pm 15$  counts/pJ over the energy range 60–900 eV. The sensitivity is expected to drop at the O and C K-edges since both elements are present in the cellulose acetate overcoat, and increase at the Br M4 and M5 edges because Br is present in the phosphor.

**Table 2.** Fits of the IP sensitivity near the C K-edge provide and estimate of the cellulose acetate areal density, assuming that the signal variation is dominated by the change in XUV absorption. Fit parameters,  $r^2$  and  $F$ , are given in the table as well.

cellulose acetate formula	areal density ( $\mu\text{g}/\text{cm}^2$ )	unattenuated sensitivity (counts/pJ)	$r^2$	$F$
$\text{C}_6\text{H}_2\text{O}_2(\text{OH})_3$	$21.0 \pm 2.3$	$32.9 \pm 1.3$	0.977	84
$\text{C}_6\text{H}_2\text{O}_2(\text{OOCCH}_3)_3$	$18.8 \pm 2.1$	$32.4 \pm 1.3$	0.976	81
average	$19.9 \pm 2.2$	$32.7 \pm 1.3$	—	—

If “mPSL” is taken to be 0.001 count, the corresponding sensitivity would be 3.4 counts/pJ, less than a factor of 10 different than what we have reported here. We consider this acceptable agreement for two IP systems employing similar technology but produced by different suppliers and operated by two different research groups.

## 4 Conclusions

We have measured the sensitivity of an image plate at XUV energies between 60 eV and 900 eV and the results look promising for imaging applications. The absorption features in the cellulose acetate overcoat only modulate the sensitivity by  $\sim 60\%$  of the peak value, and the sensitivity at 60 eV is better than 30% of the peak value. The sensitivity of the IP,  $25 \pm 15$  counts/pJ for a 600 V PMT bias and 100 micron square pixels, is compatible with 0.1 A (5 V signals recorded by a digitizer

with 50 ohm termination), 20 ns FWHM signals measured from 1 mm square photodiodes with a sensitivity of 0.2 A/W. The corresponding energy fluence,  $1 \mu\text{J}/\text{cm}^2$ , would produce a signal of 2500 counts out of a possible  $\sim 50,000$ , if the IP were scanned with 100 micron resolution. From the 600 V PMT setting used here, the bias can be varied between 300 and 1200 V to accommodate changes in the XUV source brightness.

## Acknowledgments

The authors gratefully acknowledge useful discussions with S.A. Mango, Carestream NTD, who also provided the IP that was used in this study. The Department of Energy provided the ALS beam-time and support for E.M. Gullikson. The remainder of the work was sponsored by the Defense Threat Reduction Agency (cleared for public release by the Defense Threat Reduction Agency, dated 25 January 2012, reference number NT-12-077 [PA-12-058]).

## References

- [1] B.H. Failor, N. Qi, J.S. Levine, H. Sze and E.M. Gullikson, *Soft x-ray ( $0.2 < E < 2.0 \text{ keV}$ ) imager for z-pinch plasma radiation sources*, *Rev. Sci. Instrum.* **75** (2004) 4026.
- [2] D.B. Sinars et al., *Compact, rugged in-chamber transmission spectrometers (7–28 keV) for the Sandia Z facility*, *Rev. Sci. Instrum.* **82** (2011) 063113.
- [3] A.L. Meadowcroft, C.D. Bentley and E.N. Stott, *Evaluation of the sensitivity and fading characteristics of an image plate system for x-ray diagnostics*, *Rev. Sci. Instrum.* **79** (2008) 113102.
- [4] S.A. Mango, private communication.
- [5] ALLPRO Imaging, Scan X Discover HC (Serial #1010).
- [6] L-3 Communications, “PixelRay” Image Acquisition and Analysis Software.
- [7] J.H. Underwood et al., *Calibration and standards beamline 6.3.2 at the Advanced Light Source*, *Rev. Sci. Instrum.* **67** (1996) 3372.
- [8] B.H. Failor et al., *K-shell and extreme ultraviolet spectroscopic signatures of structured Ar puff Z-pinch loads with high K-shell x-ray yield*, *Phys. Plasmas* **14** (2007) 022703.
- [9] L. Poletto, A. Boscolo and G. Tondello, *Characterization of a charge-coupled-device detector in the 1100–0.14 nm (1 eV to 9 keV) spectral region*, *Appl. Optics* **38** (1999) 29.

## **DISCLAIMER**

This document was prepared as an account of work sponsored by the United States Government. While this document is believed to contain correct information, neither the United States Government nor any agency thereof, nor The Regents of the University of California, nor any of their employees, makes any warranty, express or implied, or assumes any legal responsibility for the accuracy, completeness, or usefulness of any information, apparatus, product, or process disclosed, or represents that its use would not infringe privately owned rights. Reference herein to any specific commercial product, process, or service by its trade name, trademark, manufacturer, or otherwise, does not necessarily constitute or imply its endorsement, recommendation, or favoring by the United States Government or any agency thereof, or The Regents of the University of California. The views and opinions of authors expressed herein do not necessarily state or reflect those of the United States Government or any agency thereof or The Regents of the University of California.

This work was supported by the Director, Office of Science, of the U.S. Department of Energy under Contract No. DE-AC02-05CH11231.